Manfred Ehlers*
Institut für Photogrammetrie und Ingenieurvermessungen
Universität Hannover
D-3000 Hannover 1, Federal Republic of Germany

The Effects of Image Noise on Digital Correlation Probability

For different correlation functions, an analytical expression for the relationship of correlation probability to image signal-to-noise ratio (SNR) is derived from statistical investigations.

Introduction

In remote sensing, digital techniques are standard methods used in image processing. However, 'conventional' photogrammetry is also showing an increasing tendency towards digital image evaluation, substituting automatic components for the human operator.

One central problem is the automation of the human eye's capability, especially that of stereoscopic viewing and object identification. The digital computer controlled solution of this problem leads to the use of correlation techniques. The notation "correlation" is used in a generalized sense as a method for point or object identification. Therefore, different objective functions for the correlation process are feasible and are already in practical use (Ehlers, 1983).

The correlation process detects parallaxes, Δx and Δy, for homologous points in different images of the same area. In photogrammetry these parallaxes can be used to derive a terrain model or to produce an orthophoto; in remote sensing they serve for image rectification or change detection. For the latter case the Institute of Photogrammetry at Hannover University developed the software correlation-rectification system DISCOR (*Di*gital *s*oftware *c*orrelator for image *r*ectification) (Ehlers, 1983).

One main disadvantage in the correlation process is the possibility of incorrect parallax calculation, especially in images with a low signal-to-noise ratio (SNR). In photogrammetry the influence of image noise on correlation or pointing precision has been investigated, for example, by Förstner (1982) and Trinder (1982).

On the other hand, in remote sensing the main problem is not precision but rather the probability of the correlation function. Due to different sensors, different scales, and different recording conditions of remote sensing imagery, the identification of homologous points is very difficult. Remotely sensed images are often contaminated by noise and have to be preprocessed before further evaluation (Ehlers,

Abstract: *In remote sensing, digital correlation techniques are used to detect identical points in different images of the same area. Thus, digital correlation provides an automated technique for the determination of control points for image rectification. One disadvantage, especially in images with a low signal-to-noise ratio (SNR), is the problem of correlation failure. In this paper five different objective functions for the correlation process are compared in a statistical test on identical images with added random noise of different magnitudes. An analytical formula for the correlation probability, depending on image SNR, is derived for each objective function. Methods for SNR estimation in images with unknown noise are presented. One main result is that in images of low SNR functions other than the normal correlation function should be applied. The phase correlation method shows the highest correlation probability. With the derived relationship between correlation probability and SNR, an automatic choice of the appropriate objective function can be executed.*

* Presently with Laboratory of Remote Sensing and Mapping Science, Dept. of Geography, University of Georgia, Athens, GA 30605.

Photogrammetric Engineering and Remote Sensing,
Vol. 51, No. 3, March 1985, pp. 357-365.

0099-1112/85/5103-0357$02.25/0

FIG. 1. Aerial photography (frame camera).

1982a). An example is given in Figures 1 to 3. Figure 1 shows a photographic image (frame camera) of the city of Cologne, West Germany. Figures 2 and 3 show the same area on Landsat and Seasat imagery. The seasat radar channel, in particular, contains a high noise level.

In this paper the effects of image quality on correlation probability will be investigated in order to estimate the connection between both variables. One main aim here is to determine the correlation function with the smallest probability of failure. This is tested with five different objective functions in an empirical-statistical manner on the DISCOR system that is a part of the Hannover digital image processing system MOBI-DIVAH (Dennert-Möller *et al.*, 1982). Although the MOBI-DIVAH system was developed for remote sensing imagery, the results of the study should be applicable to other tasks such as those associated with photogrammetry.

MATHEMATICAL BASIS

IMAGE AND NOISE MODEL

In remote sensing the ground signal is changed before and during the recording process. The original image signal $g\ (x, y)$ is disturbed by various factors, e.g., the atmosphere, intensity of light, sensor sensitivity, digitization, etc. Errors due to these factors can be divided into recording (including atmospheric effects) and quantization errors. In the following we assume that atmospheric and recording processes add random noise, n', to the original signal. Thus, the recorded signal, g', can be written as

$$g'\ (x, y) = g\ (x, y) + n'\ (x, y). \tag{1}$$

Analog/digital transformation produces two effects. The finite scanning aperture size causes low pass filtering superposed with additional electronic noise (Castleman, 1979): i.e.,

$$g''\ (x, y) = g' * h''\ (x, y) + n''\ (x, y). \tag{2}$$

substituting Equation 1 into Equation 2, the digitized signal g'' can be written as

$$g''\ (x, y) = g * h\ (x, y) + n\ (x, y) \tag{3}$$

using the abbreviations $n = n' * h'' + n''$ and $h \equiv h''$.†

Hence, the digitized image signal g'' consists of a filtered deterministic part, $g * h$, and a stochastic component, n.

CORRELATION MODEL

Following Equation 3, the two independently recorded and sampled images of the same area can be written as

$$g_1'' = g * h_1 + n_1 \text{ and}$$
$$g_2'' = g * h_2 + n_2. \tag{4}$$

† The symbol '$*$' is used as an abbreviation for the convolution operator, i.e., $f * g = \int_{-\infty}^{\infty}\int_{\infty}^{\infty} f(x, y) \cdot g\ (x_0 - x, y_0 - y)\ dxdy$.

FIG. 2. Landsat MSS image.

The aim of the generalized correlation is to derive an unknown geometric transformation between g_1'' and g_2''. Usually this is done by minimizing an objective function that measures the distances between the grey values in small subimages, the correlation windows. In addition an image transformation is possible. Therefore, objective functions for the detection of identical points consist of a metric, M,† for distance measurement and a transformation parameter, T, for image preprocessing. An often used metric, for example, is the sum of squared differences between the grey values. T can change the image signal (e.g., filtering) and/or the coordinates (e.g., considering different perspectives). The task of objective function is to find Δx and Δy such that M will be minimized: i.e.,

$$M\{T(g_1''(x, y)), T(g_2''(x + \Delta x, y + \Delta y))\} = \underset{\Delta x, \Delta y}{\text{Minimum}} \quad (5)$$

OBJECTIVE FUNCTIONS

Various objective functions for the correlation process have been proposed (see, for example Göpfert (1980) and Konecny and Pape (1981)). In the evaluation of remote sensing imagery (especially from satellites), where terrain differences and perspectives can usually be neglected (Konecny, 1976), the transformation parameter T affects only the image intensities when considering no geometric conditions. With this simplification, five of these correlation functions are integrated into the DISCOR system:

(a) The 'normal' product moment correlation coefficient, which is equivalent to a square (Gaussian) metric. The transformation operator is the identity operator.

(b) The correlation intensity coefficient, which has been derived from coherent optical considerations. The image signals are mapped onto the complex plane and the intensity of the complex correlation function is computed. The coefficient is weighted by a parameter, p_1, depending on the local variances in the correlation windows. The metric, M, again is Gaussian, and the transformation operator, T, is the complex exponential.

(c) The same computation formula as in (b) is used, but with a weighting parameter, p_2, depending on the global variances in the whole images.

(d) The Laplace coefficient, i.e., the sum of the absolute differences of the image signals with an absolute (Laplacian) metric, M, and the identity operator, T.

(e) The phase correlation coefficient, i.e., the inverse Fourier transform of the normalized cross spectrum of both images. Hence, only the phase differences are considered. M again is Gaussian.

† The term "metric" is a mathematical term used for distance measurements and is defined as follows:

(1) $M(x,x) = 0$
(2) $M(x,y) = M(y,x) \neq 0$ if $x \neq y$
(3) $M(x,y) \leq M(x,z) + M(z,y)$

FIG. 3. Seasat radar image.

and T normalizes the cross spectrum in the frequency domain.

It can be shown, by using Fourier transform theorems, that the functions (a) and (e) are special cases of a generalized filtered correlation function (Ehlers, 1983). Table 1 lists the objective functions, their one dimensional unnormalized mathematical expression, the metric, M, and the transformation parameter, T. The symbols $(\cdot)^2$ and $|\cdot|$ stand for the Gaussian and Laplacian metric, respectively.

TABLE 1. MOBI-DIVAH OBJECTIVE FUNCTIONS FOR CORRELATION

Objective function	Math. expression (unnormalized)	Metric	T-Operator
(a) Productmoment correlation coefficient	$\int_{-\infty}^{\infty} g_1(x)g_2(x + \Delta x)dx$	$(\cdot)^2$	$T(g(x)) = g(x)$
(b) intensity coefficient (local variances)	$\left(\int_{-\infty}^{\infty} \cos p_1(g_1(x) - g_2(x + \Delta x))dx\right)^2$	$(\cdot)^2$	$T(g(x))$
	$+ \left(\int_{-\infty}^{\infty} \sin p_1(g_1(x) - g_2(x + \Delta x))dx\right)^2$		$= e^{-jp_1(x)g(x)}$
(c) Intensity coefficient (global variances)	as in (b) but with p_2 instead of p_1	$(\cdot)^2$	$T(g(x))$ $= e^{-jp_2g(x)}$
(d) Laplace coefficient	$\int_{-\infty}^{\infty} \lvert g_1(x) - g_2(x + \Delta x)\rvert dx$	$\lvert\cdot\rvert$	$T(g(x)) = g(x)$
(e) Phase correlation coefficient	$\int_{-\infty}^{\infty} \frac{G_1^*(f)G_2(f)}{\lvert G_1(f)G_2(f)\rvert} e^{2\pi jf\Delta x}df$	$(\cdot)^2$	$T(G(f)) = \frac{G(f)}{\lvert G(f)\rvert}$

($G(f)$ = Fourier transform of $g(x)$: $G(f) = \int_{-\infty}^{\infty} g(x) \cdot e^{-2\pi jfx}dx$ with $j = \sqrt{-1}$).

Of great importance is the classification of the objective functions. Which criteria can be used for classification? Applicable criteria may be precision, sensitivity, convergence, computation time, and probability against gross errors. We chose the last one as the most applicable. Because what is the value of the fastest, most sensitive, and precise function, if it is at the wrong point? Therefore, in the following section the correlation probability is studied using statistical tests with different artificial noise distributions.

Correlation Probability and SNR

IMAGE MATERIAL

As a test image, a digitized section of an aerial photograph with an original scale of 1:50 000 was chosen (Figure 4). Due to the high SNR in photo-graphic pictures, this image is used to simulate an undisturbed original ground signal. It is assumed to be noise-free. Now random noise of different magnitudes and distributions is added to the reference signal according to Equation 3. The mean SNR in the noisy images can be estimated from

$$\overline{SNR} = \frac{\overline{\sigma_g}}{\sigma_n} \tag{6}$$

where $\overline{\sigma}_g$ is the mean value for the standard deviation of the image signal and $\overline{\sigma}_n$ is the random noise mean standard deviation.

Table 2 shows SNR and noise distribution in the 20 different noisy test images.

Figures 5 and 6 show two noisy images with an SNR = 2.6 and 1.0, respectively. The differences can be seen more clearly in Figure 7, which shows the same line in the reference image and the two disturbed images.

In the reference image, 20 correlation test points have been chosen on the digital DIVAH screen. The correlation points are the centers of 11 by 11 pattern matrices. In the noisy images the corresponding search matrices have the same center coordinates and a size of 30 by 30 pixels. Within these windows the correlation coefficients for all possible pattern matrix positions are computed. With the *a-priori* knowledge for correct correlation, we can estimate the correlation probability for every objective function (Ehlers, 1983). Figure 8 shows the reference image with the outlined pattern matrices.

Table 2. SNR and Noise Distribution

SNR	Distribution*
60.8	G
50.7	U
30.4	G
21.7	U
15.2	G
10.5	U
10.1	G
5.2	U
3.5	U
3.0	G
2.6	U
2.3	U
2.1	U
2.0	G
1.8	U
1.5	G
1.3	U
1.2	G
1.0	G
0.8	G

* G = Gaussian distributed. U = Uniform distributed.

TEST RESULTS

The correlation test shows no significance on the applied kind of noise distribution; therefore, we can

Fig. 4. Reference image (noisefree).

Fig. 5. Search image (SNR = 2.6).

FIG. 6. Search image (SNR = 1.0).

FIG. 8. Reference image with outlined correlation points.

combine all the results. Only the SNR values are considered. The SNR is computed in every correlation window and summarized in 18 different SNR classes. In each class the correlation probability for every objective function is calculated. The results can be seen in Table 3. A probability of 0.5, for example, means that 50 percent of the correlation points in the corresponding SNR class have been recognized correctly.

For an easier interpretation, it is convenient to develop a mathematical expression of the relationship between probability and SNR.

MATHEMATICAL APPROXIMATION OF CORRELATION PROBABILITY AND SNR

To obtain an analytical expression for the connection between noise and correlation probability, P, the P-values are plotted versus the corresponding logarithmic SNR. We get an S-shape curve with an almost linear increase in the medium domain (see Figure 9). For an analytical formulation, we have to approximate the probability functions considering the boundary conditions

$$\lim_{\text{SNR}\to 0} p = 0$$

and

$$\lim_{\text{SNR}\to \infty} p = 1$$

An easy analytical solution can be given by the 'logistic growth curve'

$$y = \frac{1}{1 + e^{-a_1 x - a_0}} \tag{7}$$

which was set up first by Volterra for population processes (Whiston, 1974).

For the estimation of the parameters a_0 and a_1, we consider the expression

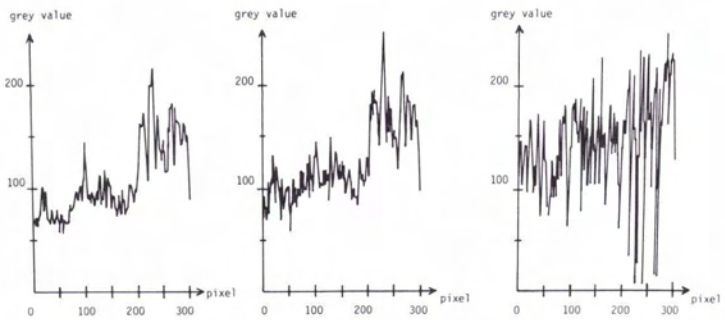

FIG. 7. Line in reference image (left), image with SNR = 2.6 (center), and image with SNR = 1.0 (right).

TABLE 3. CORRELATION PROBABILITY AND SNR

SNR from-to	SNR	Number of correlation points	Probability with objective function* a	b	c	d	e
0.07-0.10	—	2	0.00	0.00	0.00	0.00	0.00
>0.10-0.15	0.13	14	0.00	0.00	0.00	0.00	0.36
>0.15-0.20	0.18	17	0.06	0.00	0.12	0.00	0.47
>0.20-0.27	0.25	18	0.44	0.00	0.17	0.00	0.67
>0.27-0.33	0.31	16	0.44	0.19	0.38	0.00	0.63
>0.33-0.40	0.39	16	0.57	0.43	0.57	0.00	0.93
>0.40-0.45	0.43	14	0.71	0.79	0.79	0.00	0.86
>0.45-0.50	0.49	13	0.62	0.62	0.69	0.15	0.77
>0.50-0.60	0.57	17	0.88	0.88	0.94	0.06	1.00
>0.60-0.70	0.66	17	0.88	0.88	0.88	0.00	0.94
>0.70-0.80	0.76	12	1.00	1.00	1.00	0.17	1.00
>0.80-0.90	0.86	17	0.94	1.00	1.00	0.24	1.00
>0.90-1.00	0.96	12	0.92	0.75	1.00	0.25	1.00
>1.00-1.50	1.25	46	1.00	1.00	1.00	0.33	1.00
>1.50-2.00	1.75	24	1.00	1.00	1.00	0.63	1.00
>2.00-5.00	3.50	56	1.00	1.00	1.00	0.95	1.00
>5.00-10.00	7.50	42	1.00	1.00	1.00	0.98	1.00
>10.0		36	1.00	1.00	1.00	1.00	1.00

* a = Product moment correlation coefficient
b = Intensity coefficient (local variances)
c = Intensity coefficient (global variances)
d = Laplace coefficient
e = Phase correlation coefficient

$\log \frac{y}{1-y}$ of Equation 7: i.e.,

$$\log \frac{y}{1-y} = \log y - \log (1-y) = a_1 x + a_0$$

or, in our case,

$$\log \frac{P}{1-P} = a_1 \log \text{SNR} + a_0. \qquad (8)$$

Figure 9 shows the approximated curves P(SNR) for all objective functions according to Equation 8. Also, their 95 percent confidence interval and the measured probabilities, $\hat{p}$, are plotted. The significance of the fits has been verified by chi-square testing.

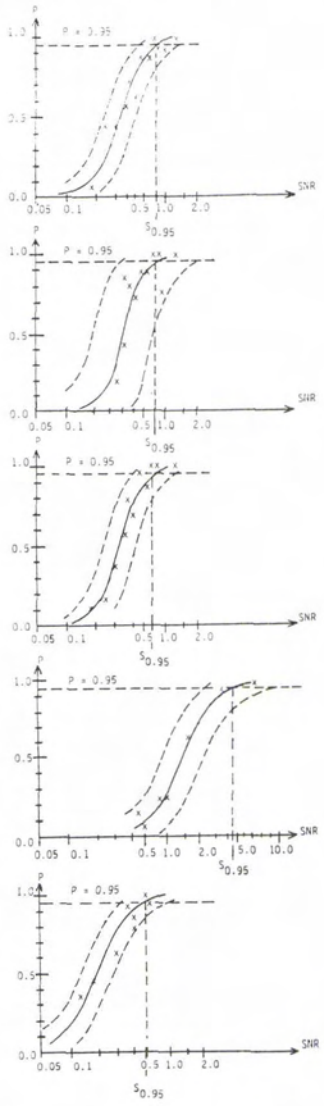

FIG. 9. Probability and SNR of product moment correlation coefficient (a), intensity coefficient (b), intensity coefficient (c), Laplace coefficient (d), and phase correlation coefficient (e) (from top to bottom).

OBJECTIVE FUNCTION CLASSIFICATION

To classify the correlation functions, limiting values are extracted from Figure 9. The parameter $S_{0.05}$, $S_{0.50}$, and $S_{0.95}$ denote the SNR with a probability of 5 percent, 50 percent, and 95 percent, respectively. Table 4 presents the estimated parameters with their upper 95 percent confidence interval.

The classification criteria listed in Table 4 allow us to come to the following conclusions:

- The best correlation probability is shown by the phase correlation method (e). A SNR of 1.5 or lower in our images requires the application of this objective function to achieve the most probable correlation.
- The objective functions (a) and (c) have almost the same probability of correct correlation showing no significant differences. Therefore, other criteria, such as those listed in the correlation model section, may decide which one has to be used. If the image SNR is above 1.5, functions (a), (b), (c), and (e) can be employed without preference.
- The correlation intensity function (b) has almost the same formula and an identical theoretical background as function (c). However, (b) shows worse results in all SNR parameters when compared with (c). Therefore, it can be neglected in the correlation process.
- A poor probability is associated with function (d), the Laplace coefficient. Incorrect correlation occurs even at an image SNR of 9.0. Although a very fast function (Ehlers, 1982b), it shows insufficient

TABLE 4. SNR VALUES WITH P = 0.05, AND 0.95

Objective function	$S_{0.05}$	95% confidence	$S_{0.50}$	95% confidence	$S_{0.95}$	95% confidence
a	0.14	0.24	0.34	0.50	0.82	1.40
b	0.18	0.50	0.38	0.78	0.80	2.00
c	0.15	0.26	0.34	0.40	0.76	1.25
d	0.42	0.76	1.40	2.20	4.60	12.00
e	0.06	0.12	0.19	0.28	0.50	1.00

probability and should therefore be handled with care in the correlation process.

With these limiting values, it is possible to control the application of objective functions in an automatic manner. If the SNR is known, it is possible to decide which correlation function can be chosen and to estimate its *a-priori* correlation probability. Thus, the image SNR is all that an automatic correlation controller needs to know. But how can it be calculated if image and noise are almost inseparable?

ESTIMATION OF IMAGE SNR

The crucial point of such an investigation is to find a good SNR estimation because, normally, the intensity and distribution of noise is unknown. Therefore, simplifying assumptions must be made to derive SNR values from noisy image signals.

A-posteriori SNR estimation can be done using the values of maximum correlation of grey level differences (Förstner, 1982; Trinder, 1982) but, by doing so, we cannot avoid incorrect correlation. Therefore, we need an *a-priori* noise estimation.

SNR estimation per correlation point. Typical power spectra of aerial photographs show an exponential decrease with increasing frequency (Helava, 1978): i.e.,

$$P_g(f) = P_g(0) \cdot e^{-a|f|} \tag{9}$$

$P_g(f)$ is the power spectrum of the image signal g at the frequency f, which can be measured in lines or linepairs per mm. The parameter $a > 0$ is an image specific constant.

We assume that all superimposed disturbance effects can be regarded as white noise n, i.e., having a constant power spectrum

$$P_n(f) = N_0^2 \tag{10}$$

where P_n is the noise power spectrum, and N_0^2 is the constant intensity. The power spectrum of image and noise is shown in Figure 10.

The variances σ_n^2 for noise and σ_g^2 for the image can be estimated by

$$\sigma_n^2 = N_0^2$$

$$\sigma_g^2 = 2P_g(0) \cdot \int_0^\infty e^{-af}\, df = 2P_g(0)/a.$$

Thus, the SNR is calculated as

$$\text{SNR} = \sqrt{\frac{2\,P_g(0)}{a \cdot N_0^2}}\,. \tag{11}$$

Using Equation 11, the SNR can be computed in every correlation window, and P can be estimated from Equation 8. But the calculation of N_0^2 and a is time consuming, requiring a Fourier transformation and user interaction. However, the DISCOR system allows an easier and faster way for SNR estimation.

Global SNR estimation. Again, noise is assumed to be white and also constant over the whole image. Thus, σ_n^2 can be estimated in a representative image area according to Equation 10. This σ_n^2 is considered to be valid for all correlation windows. Image and noise can be regarded as independent stochastic variables. Hence, the variance, σ_g^2, of the undisturbed signal, g, can be calculated as the difference between $\sigma_{g'}^2$, the variance of the disturbed signal g', and σ_n^2: i.e.,

$$\sigma_g^2 = \sigma_{g'}^2 - \sigma_n^2 = \sigma_{g'}^2 - N_0^2$$

So a simple variance computation in a correlation window yields the corresponding SNR:

$$\text{SNR} = \sqrt{\frac{\sigma_{g'}^2 - N_0^2}{N_0^2}}\,. \tag{12}$$

Equation 12 is used to estimate the *a-priori* probability, P, to avoid incorrect correlation.

CONCLUSIONS

With the presented formulas for correlation probability and image SNR, an *a-priori* estimation of the expected correlation accuracy can be given. Based on the image quality in a correlation window, it is possible to decide which objective function should be used and to calculate the probability of correct (or incorrect) correlation.

If a correlation point shows too low an SNR, it can be neglected or the SNR (and the correlation probability) can be increased by low pass filtering or by extending the correlation window (Ehlers, 1983). Based on Equation 8, correlation probability is a function of only *one* variable: the SNR. All known methods to raise correlation probability, e.g., filtering or enlargement of the correlation window, are accomplishing nothing more than increasing the local SNR at the correlation point.

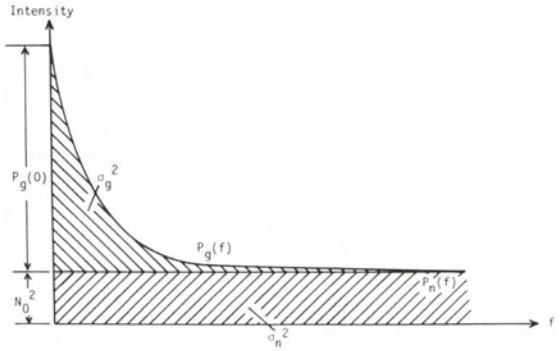

FIG. 10. Power spectrum of image and noise.

The values of the correlation maxima have no influence on the correlation probability. This corresponds with previous results (Ehlers, 1982a).

Naturally, this study tries to answer only one question about correlation quality. Simplifying assumptions for noise and signal have had to be made in order to derive an analytical expression for probability and SNR. Geometrical differences have not been considered and different quantization errors have not been investigated. Finally, the definition of SNR includes only the image variances, neglecting such important features as texture parameters, edge direction, significant patterns, etc. Therefore, the SNR definition should be generalized in this sense.

Thus, Equation 8 is just one mosaic stone of a sufficient mathematical description of something the human eye can solve in an unconscious way. One result of this paper is that we must consider objective functions other than solely the normal correlation coefficient. The phase correlation method shows less susceptibility to low SNR and should, therefore, be applied in noisy images. So future correlation systems should be open to include these and prospective results. They should contain the opportunity to generalize the objective function, i.e., the metric and the transformation operator. Also, picture preprocessing and variable choice of window size should be feasible. This is only possible with a software solution conveniently embedded into a digital image processing system.

REFERENCES

Castleman, K., 1979. *Digital Image Processing*, Prentice-Hall, 429 p.

Dennert-Möller, E., M. Ehlers, D. Kolouch, and P. Lohmann, 1982. Das digitale Bildverarbeitungssystem MOBI-DIVAH, *Bildmessung und Luftbildwesen* 50, pp. 201-203.

Ehlers, M., 1982a. Increase in Correlation Accuracy by Digital Filtering, *Photogrammetric Engineering and Remote Sensing*, Vol. 48, pp. 415-420.

———, 1982b. Digital Image Processing of Remote Sensing Imagery: A Comparative Study on Different Functions in Correlation Process, *Proc. of the Intern. Symp. Comm. VII, ISP*, Toulouse, pp. 71-77.

———, 1983. *Untersuchungen von digitalen Korrelationsverfahren zur Entzerrung von Fernerkundungsaufnahmen*, Wissenschaftliche Arbeiten der Fachrichtung Vermessungswesen der Universität Hannover, Dissertation, 247 p.

Förstner, W., 1982. On the Geometric Precision of Digital Correlation, *Proc. of Comm. III, ISP*, Helsinki, pp. 176-189.

Göpfert, W., 1980. Image Correlation and Change Detection, *Proc. of XIVth Congress of ISP*, Vol. 23/B3, Comm III, pp. 246-255.

Helava, U. V. 1978. Digital Correlation in Photogrammetric Instruments, *Photogrammetria* 34, pp. 19-41.

Konecny, G., 1976. Mathematical Models and Procedures for the Geometric Restitution of Remote Sensing Imagery, *Working Group Rep. III.1*, XIIIth Congress of ISP, Helsinki.

Konecny, G., and D. Pape, 1981. Correlation Techniques and Devices, *Photogrammetric Engineering and Remote Sensing*, Vol. 47, pp. 323-333.

Trinder, J. C., 1982. The Effects of Photographic Noise on Pointing Precision, Detection, and Recognition, *Photogrammetric Engineering and Remote Sensing*, Vol. 48, pp. 1563-1575.

Whiston, T. G., 1974. *Life is Logarithmic. Advances in Cybernetics and Systems*, Gordon and Breach.

(Received 30 April 1983; revised and accepted 18 November 1984)